Reliability Analysis and Performance Degradation of a Boost Converter

Mohammed Khorshed Alam, *Student Member, IEEE*, and Faisal H. Khan, *Senior Member, IEEE*

Abstract—In general, power converters are operated in closed-loop systems, and any characteristic variations in one component will simultaneously alter the operating point of other components, resulting in a shift in overall reliability profile. This interdependence makes the reliability of a converter a complex function of time and operating conditions; therefore, the application may demand periodic replacement of converters to avoid downtime and maintenance cost. By knowing the present state of health and the remaining life of a power converter, it is possible to reduce the maintenance cost for expensive high-power converters. This paper presents a reliability analysis for a boost converter, although this method could be used to any power converter being operated using closed-loop controls. Through the conducted study, it is revealed that the reliability of a boost converter having control loops degrades with time, and this paper presents a method to calculate time-varying reliability of a boost converter as a function of characteristic variations in different components in the circuit. In addition, the effects of operating and ambient conditions have been included in the reliability model as well. It was found that any increase in the ON-state resistance of the MOSFET or equivalent series resistance of the output capacitor decreases the overall reliability of the converter. However, any variation in the capacitance has a more complex impact on the converter's reliability. This paper is a step forward to the power-converter reliability analysis because the cumulative effect of multiple degraded components has been considered in the reliability model.

Index Terms—Closed-loop systems, condition monitoring, failure analysis, reliability theory, switch-mode dc–dc converters.

I. INTRODUCTION

THE reliability and failure study of individual components used in power converters has been well conducted and can be found in literature [1]–[4]. A bathtub curve of the failure rate is the most accepted model for any electronic component [5], [6], and this curve is shown in Fig. 1(a). The infant failure of the components is generally linked to poor design, poor installation, or misapplication, and a constant failure rate defines the useful lifetime of the component. However, several disagreements with the bathtub curve have been presented in
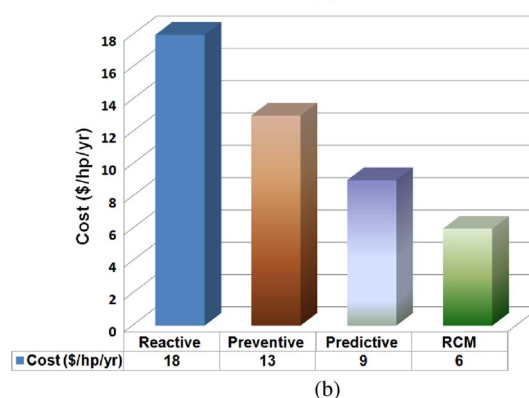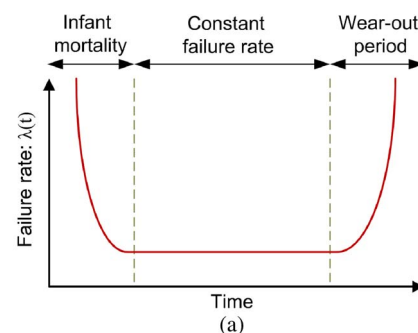
Fig. 1. (a) Bathtub curve for the component failure rate. (b) Cost analysis for different maintenance schemes applied to electric pumps [5]–[7].

different studies [8], [9]. According to our conducted study, this constant failure rate changes due to any characteristic variation of the components because of the aging involved with the entire power converter. Therefore, a proper maintenance program is required to ensure a safe, efficient, and effective operation of a system having power converters.

Reactive maintenance is the most dominant type of maintenance program in industry, and in this method, all converters and drives are allowed to run until they fail. Any replacement/repair is performed after the failure occurs. This results in the highest downtime cost and may damage other components in the system. Other maintenance schemes attempt to predict the failure of any component and replace/repair the components before any failure takes place. A relative cost analysis for different pump maintenance schemes is shown in Fig. 1(b) [5]–[7], and the reliability-centered maintenance is the most efficient maintenance program, although it requires a sophisticated prognostics and diagnosis technique.

Power converters are used in a wide variety of applications, and some applications requires very high reliability such as commercial and military aircraft, space applications, etc. [10]. Moreover, the relevant cost of failure of a converter can be
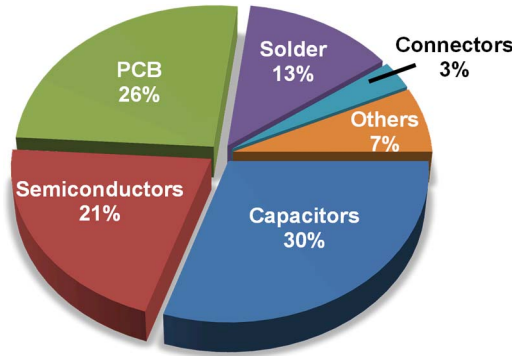
Fig. 2. Survey of different fragile components responsible for converter failure [19].

Fig. 3. Schematic of the closed-loop boost converter.

TABLE I
CIRCUIT PARAMETERS OF THE BOOST CONVERTER

Symbol	Description	Value
V_{in}	Input voltage	40 V
V_{out}	Output voltage	100 V
L	Inductance	1 mH
r_L	Equivalent series resistance (ESR) of the inductor	0.1 Ω
$R_{DS(ON)}$	MOSFET ON resistance	0.034 - 0.044 Ω
r_D	Diode on resistance	0.05 Ω
V_f	Diode forward voltage	0.5 V
C	Output capacitance	5-10 μF
ESR	ESR of the capacitor	0.1-0.18 Ω
R_{out}	Output load resistance	50 Ω
f_{sw}	Switching frequency	10 kHz
P_{rated}	Rated power of the converter	215 W

higher than 80% of the system cost in some highly integrated products, which are intended to be maintenance free [11]. Therefore, a safe estimation of reliability of these converters would be crucial in those cases. However, standards for estimating the failure rates of power converters are still evolving and often referred to the military handbook MIL-HDBK-217F [2], [10], [12]–[16]. Reliability-centered design of power converters require prior knowledge of failure mode, mechanism, and effect analysis (FMMEA) of different components, and a guideline for reliability-centered design has been provided in [10] and [17]–[20].

Most of the power converters are being operated in a closed-loop system in order to maintain expected voltage and currents at different nodes. The control system also protects the converter from any potential overload or short circuit. Therefore, the operating condition of a power converter is affected by any variation in components' electrical parameters, input/output loading, and ambient conditions. Any characteristic variation in one component will simultaneously affect the operating condition and the corresponding thermal stress. This may accelerate the aging process of that component and the remaining components of the converter.

It is important to identify the failure-prone components and corresponding parameters that need to be monitored for designing an effective prognostics and health management (PHM) scheme of a power converter. Cheng *et al.* have described the process of identifying a potential failure precursor of a component in terms of FMMEA [20]. Yang has reported a survey on reliability of power converters and provided statistics on fragile components used in power converters, as shown in Fig. 2 [11], [23]. Different condition monitoring techniques of power switches are well explained and compared in [24]. In addition, monitoring different converter electrical characteristics require *in situ* measurement of different parameters such as temperature, vibration, voltage, current, magnetic fields, etc. Pecht summarized the common sensors and their sensing principles used in PHM for different systems in [19].

It is widely accepted that power switches and capacitors are the most failure-prone components in a power converter [11], [17], [21]–[25]. In this regard, variation in the reliability function as a function of MOSFET's ON-state resistance $R_{DS(ON)}$, capacitance C, and the equivalent series resistance (ESR) of
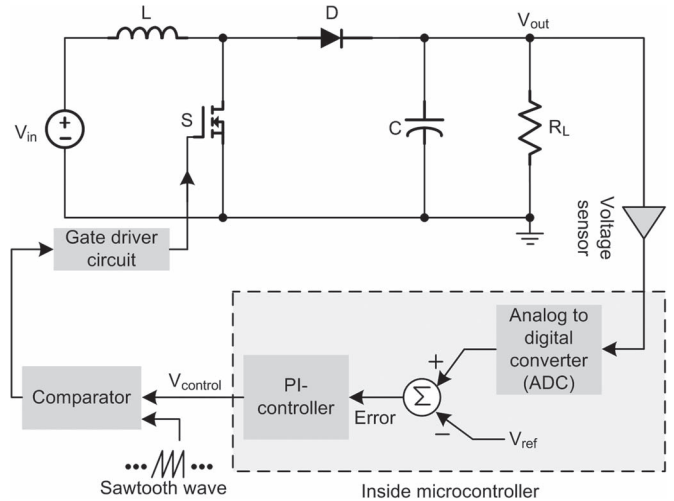
the capacitor in a closed-loop boost converter circuit has been analyzed in this paper.

A simple boost converter with a feedback control loop intended to maintain only the output voltage (no current control) has been considered in this paper. The voltage conversion ratio (CR) of an ideal boost converter operating in continuous conduction mode (CCM) is related to the duty ratio (d) of the gate signal, as shown in (1) as follows:

$$\text{CR} = \frac{V_{\text{out}}}{V_{\text{in}}} = \frac{1}{1-d}. \tag{1}$$

Detail analysis of this well-known topology can be found in [26] and [27]. A schematic of the boost converter is shown in Fig. 3, and various circuit parameters are listed in Table I. Although different control techniques for switched-mode power converters have been proposed in literature, a simple proportional–integral (PI) controller has been considered here to control the output voltage of the converter using duty ratio control [28]–[34].

It has been shown in [2] that increased MOSFET's ON-state resistance of an interleaved boost converter operating in

an open-loop system increases the reliability of the converter due to a decrease in output voltage across the capacitor. However, this analysis cannot be applied to boost converters being operated in closed loop and therefore needs modifications to accommodate the closed-loop operation of the converter. To the best of our knowledge, no analysis has been presented yet to address the reliability degradation of any closed-loop power converters.

II. RELIABILITY ESTIMATION OF A BOOST CONVERTER

Reliability estimation of a boost converter based on MIL-HDBK-217F considering no variation of characteristic parameters of components is presented in this section, and all the equations have been organized for a better presentation.

Considering a constant failure rate λ_{SYSTEM0}, reliability of the system can be calculated as shown in (2) [1], [3] as follows:

$$R_s(t) = e^{-(\lambda_{\text{SYSTEM}} \times t)} \tag{2}$$

where $R_S(t)$ is the probability of having no failure within duration of t. The mean time to failure (MTTF) can be calculated from the reliability probability function shown in (3) as follows:

$$\text{MTTF} = \int_0^\infty R_s(t)dt = \frac{1}{\lambda_{\text{SYSTEM}}} \tag{3}$$

and the failure rate of an N-channel MOSFET can be written as (4) [1] as follows:

$$\lambda_{\text{SW}} = \lambda_B \pi_T \pi_A \pi_E \pi_Q. \tag{4}$$

The base failure rate λ_B has a constant value of 0.012, and the application factor π_A and quality factor π_Q are both equal to 8 for switches rated at 135 W. Environmental factor π_E is considered 9 for equipment installed on wheeled or tracked vehicles [1]. Temperature factor and junction temperature can be calculated using (5) as follows:

$$\pi_T = \text{temperature factor}$$

$$= \exp\left[-1925\left(\frac{1}{T_J + 273} - \frac{1}{298}\right)\right]$$

$$T_J = T_a + (\theta_{\text{JA}})P_{\text{SW}} \tag{5}$$

with ambient temperature T_a set to 25 °C and junction-to-ambient thermal resistance θ_{JA} is set to 18 °C/W for D2PAK packaging [37]. The total power dissipation (conduction loss plus switching loss) of the switching device is P_{SW}. Considering the values stated earlier, the failure rate of the MOSFET can be calculated using (6)

$$\lambda_{\text{SW0}} = \lambda_B \pi_T \pi_A \pi_E \pi_Q$$

$$= 0.012 \times \pi_T \times 8 \times 9.0 \times 8$$

$$= 6.912 \times \pi_T \tag{6}$$

and considering that the power loss (conduction loss plus switching loss) in a switch is 1.3532 W, the failure rate of the

MOSFET is calculated as in (7) as follows:

$$T_J = T_a + (\theta_{\text{JA}})P_{\text{SW}} = 25 + (18 \times 1.3532)$$

$$= 49.3576$$

$$\pi_T = \exp\left[-1925\left(\frac{1}{T_J + 273} - \frac{1}{298}\right)\right] = 1.6292$$

$$\lambda_{\text{SW0}} = 6.912 \times 1.6292$$

$$= 11.2610 \text{ failure/million hours.} \tag{7}$$

Similar analysis can be performed for the inductor, diode, and capacitor. For the boost converter under consideration, the failure rate and MTTF of the converter is shown in (8) and (9), respectively, as follows:

$$\lambda_{\text{SYSTEM0}}$$

$$= \lambda_{\text{SW0}} + \lambda_{\text{CAP0}} + \lambda_{\text{DIODE}} + \lambda_{\text{INDUCTOR0}}$$

$$= 6.912 \times \exp\left[-1925\left(\frac{1}{T_a + (\theta_{\text{JA}})P_{\text{SW}} + 273} - \frac{1}{298}\right)\right]$$

$$+ 120 \times \left(0.0028 \times \left[\left(\frac{S_{\text{CAP}}}{0.55}\right)^3 + 1\right]\right.$$

$$\left. \times \exp\left(4.09 \times \left(\frac{T + 273}{358}\right)^{5.9}\right)\right)$$

$$\times 0.495621 + 0.01166$$

$$\times \exp\left[-3091\left(\frac{1}{T_a + (\theta_{\text{JA}})P_{\text{diode}} + 273} - \frac{1}{298}\right)\right]$$

$$+ 0.00108 \times \exp\left[-\frac{0.11}{8.617 \times 10^{-5}}\left(\frac{1}{T_{\text{HS}} + 273} - \frac{1}{298}\right)\right]$$

$$= 11.2610 + 4.2600 + 0.0283 + 0.9225$$

$$= 16.4718 \text{ failure/million hours} \tag{8}$$

$$\text{MTTF}$$

$$= \frac{1}{\lambda_{\text{SYSTEM}}} = \frac{10^6}{16.4718} \text{ hours/failure}$$

$$= 6.930 \text{ years/failure.} \tag{9}$$

III. EFFECT OF VARIATION IN DIFFERENT COMPONENT PARAMETERS

Variation of the reliability function as a function of any change in MOSFET's ON-state resistance $R_{DS(\text{ON})}$, capacitance C, and the ESR of the capacitor in a simple boost converter circuit operated in a closed loop will be analyzed in this section.

Effect of Any Variation in $R_{DS(\text{ON})}$

Any increase in $R_{DS(\text{ON})}$ of a MOSFET is the dominant precursor of failure for a power MOSFET [21], [22], and variation in $R_{DS(\text{ON})}$ has been well studied in several works [4], [35], [36]. For a fixed gate-to-source voltage, the $R_{DS(\text{ON})}$ of the MOSFET depends on the present value of $R_{DS(\text{ON})}$, temperature, and the power loss in the MOSFET. Any increase in the value of $R_{DS(\text{ON})}$ will affect the thermal stress on the switch, increase the junction temperature, change the operating point of the converter, and decrease the reliability according to (5), and this corresponding effect is shown in Fig. 4(a).

The failure rate of the MOSFET can be updated as shown in (10) as follows:

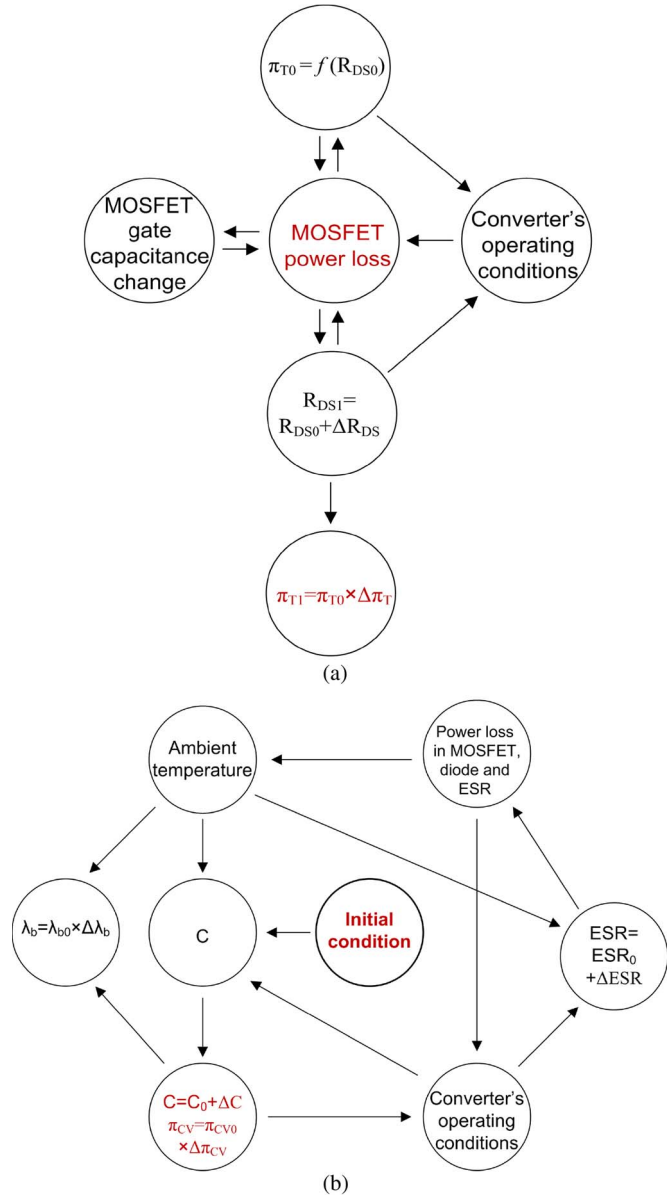$$\lambda_{\text{SW}}(t) = \lambda_{\text{SW0}} \times f_1(\Delta R_{\text{DS}}) \tag{10}$$

Fig. 4. (a) Effect of $R_{DS(\mathrm{ON})}$ variation of the MOSFET on the reliability of the converter. (b) Effect of capacitance C and ESR variations on the reliability of the converter.

where λ_{SW0} is the failure rate of the MOSFET considering that there is no change in $R_{DS(\mathrm{ON})}$ over time. Function f_1 depends on the change in MOSFET's ON-state resistance. In addition,

increased thermal stress changes the gate capacitance of the MOSFET, which may cause degraded switching performance, and it may result in higher thermal stress because of the elevated switching loss. Therefore, reliability of a switch is highly dependent on the prolonged operation of the converter and cannot be accurately predicted by assuming a constant rate of failure.

Change in Capacitance C and ESR

A state diagram for characteristic variation of a capacitor used in a power converter is shown in Fig. 4(b). Both the base failure rate and the capacitance have been considered time-varying in this model. The time-dependent failure rate of the capacitor is shown in (11) as follows:

$$\pi_{\mathrm{CV}}(t) = \pi_{\mathrm{CV0}} \times \Delta\pi_{\mathrm{CV}} = \pi_{\mathrm{CV0}} \times f_2(\Delta C)$$
$$\lambda_b(t) = \lambda_{b0} \times \Delta\lambda_b$$
$$= \lambda_{b0} \times f_3(\Delta C, T_a,$$
$$\Delta T_{\mathrm{power\_loss\_in\_MOSFET\_diode,and\_ESRs}})$$
$$\lambda_{\mathrm{CAP}}(t) = \lambda_{\mathrm{CAP0}} \times f_2 \times f_3 = \lambda_{\mathrm{CAP0}} \times f_4. \tag{11}$$

π_{CV0} and λ_{b0} are the capacitance factor and the base failure rate of the capacitor, considering no variation in capacitance over time.

Gradual change/degradation in capacitance depends on the type of capacitor used, and this change is highly dependent on the ambient temperature. Thermal stress is the dominant factor for electrolytic capacitor failure, and power loss in other components (MOSFET, diode, ESR of the inductor, and ESR of the capacitor itself) may increase the ambient temperature of the capacitor. Output voltage ripple increases with any decrease in capacitance, and it increases the voltage stress in the capacitor as well. Higher voltage and ripple current stress play significant roles to increase the ESR, and any increase in ESR results in higher power loss and ambient temperature rise [38], [39]. f_1, f_2, and f_3 are the unknown functions and need to be identified.

Let us consider the boost converter shown in Fig. 3. The following analysis will consider variations in device parameters and define reliability of the converter as a time-varying function. Therefore, the failure rate of the converter $\lambda_{\mathrm{SYSTEM}}$ and MTTF will no more be a constant and can be expressed as shown in (12), shown at the bottom of the page.

$$\lambda_{\mathrm{SYSTEM}}(t) = \lambda_{\mathrm{SW}}(t) + \lambda_{\mathrm{CAP}}(t) + \lambda_{\mathrm{DIODE}}(t) + \lambda_{\mathrm{INDUCTOR}}(t)$$

$$\mathrm{MTTF} = \int_0^\infty R_s(t)dt = \int_0^\infty e^{-(\lambda_{\mathrm{SYSTEM}}(t) \times t)}dt \neq \frac{1}{\lambda_{\mathrm{SYSTEM}}(t)}$$

$$\mathrm{MTTF} = \int_0^\infty e^{-(\lambda_{\mathrm{SW}}(t) + \lambda_{\mathrm{CAP}}(t) + \lambda_{\mathrm{DIODE}}(t) \times t + \lambda_{\mathrm{INDUCTOR}} \times t)}dt$$

$$= \int_0^\infty e^{-(\lambda_{\mathrm{SW}}(t) \times t)} e^{-(\lambda_{\mathrm{CAP}}(t) \times t)} e^{-(\lambda_{\mathrm{DIODE}}(t) \times t)} e^{-(\lambda_{\mathrm{INDUCTOR}}(t) \times t)}dt \tag{12}$$
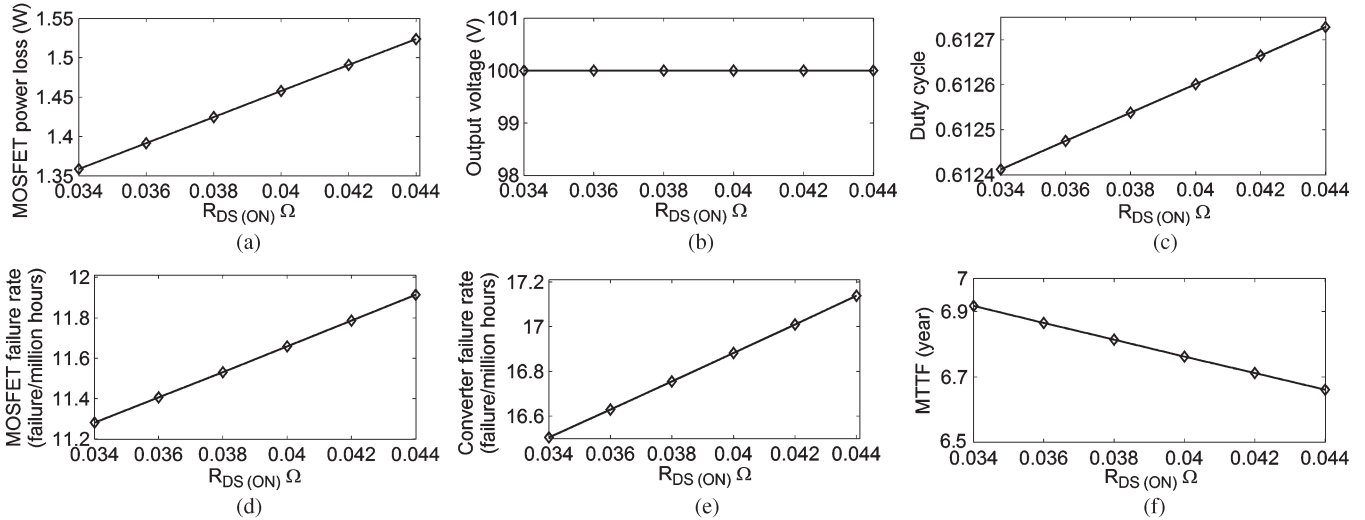
Fig. 5. Effect of $R_{DS(ON)}$ variation on the operating condition and reliability of the closed-loop boost converter. (a) Variation in power loss in the MOSFET. (b) Output voltage. (c) Duty cycle variation. (d) Failure rate of the MOSFET. (e) Converter failure rate. (f) MTTF of the converter as a function of $R_{DS(ON)}$.
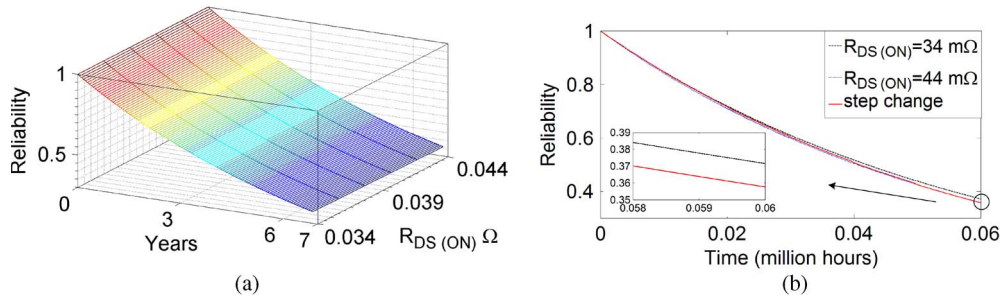

Fig. 6. (a) Reliability probability function of a closed-loop boost converter for the variation in $R_{DS(ON)}$. (b) Reliability probability function variation for step change in $R_{DS(ON)}$.

This approach works for circuits with a limited number of components, and this is why the reliability analysis of power converters could be benefited from this method. An initial reliability of a converter can be estimated based on the measurable quantities such as $R_{DS(ON)}$, ESR, C, and so on, and it can be updated periodically by measuring those parameters with a regular interval. Variation of the reliability function with the variation in $R_{DS(ON)}$, C, and ESR of the closed-loop boost converter is presented in Section IV.

IV. SAMPLE RELIABILITY MODEL: A TEST CASE

The reliability of the closed-loop boost converter for the change in MOSFET's ON-state resistance from 34 to 44 mΩ, in capacitance variation from 5 to 10 μF, and in ESR variation from 0.1 to 0.18 Ω will be presented here.

Change in MOSFET ON-State Resistance $R_{DS(ON)}$

The boost converter shown in Fig. 3 has been simulated in PSIM, and the results have been imported to MATLAB to calculate the reliability. The feedback controller was implemented using a simple PI controller with a gain of 0.1, and the time constant was set to 0.001. Output capacitor's capacitance and ESR were set to 10 μF and 0.1 Ω, respectively. $R_{DS(ON)}$ of the MOSFET was varied from 34 to 44 mΩ. This variation of ON-state resistance is consistent with the experimental data reported

in [22] (as a result of accelerated thermal aging process of a MOSFET).

The simulation results are shown in Fig. 5. Fig. 5(a) shows that power loss in the MOSFET (sum of the switching and conduction loss) increases with any increase in the ON-state resistance, and Fig. 5(b) and (c) shows the output voltage and duty cycle of the converter, respectively. The PI controller maintains a fixed output voltage by changing the duty ratio to compensate for any variation in $R_{DS(ON)}$. The failure rate of the MOSFET increases with any increase in $R_{DS(ON)}$ due to increased thermal stress and thereby increases the failure rate of the converter as well. These are shown in Fig. 5(d) and (e), respectively. It should be noted that increased $R_{DS(ON)}$ in a closed-loop system do not increase the reliability of the converter as opposed to the open-loop system discussed in [2]. The MTTF of the converter is reduced by about 2238 h (0.2556 years) for the variation in $R_{DS(ON)}$ from 34 to 44 mΩ, and this is shown in Fig. 5(f).

Reporting a real-time characteristic variation of a power converter may take years of continuous observation in a controlled ambient condition, and this is not feasible. Therefore, a test case is considered here. Assuming a rate of increase in $R_{DS(ON)}$ of 2 mΩ/10 000 h, the results are plotted in Fig. 6. There is about 3.75% variation in reliability after 60 000 h of operations or 2238-h variation in MTTF if the variation in MOSFET's ON-state resistance is taken into account.
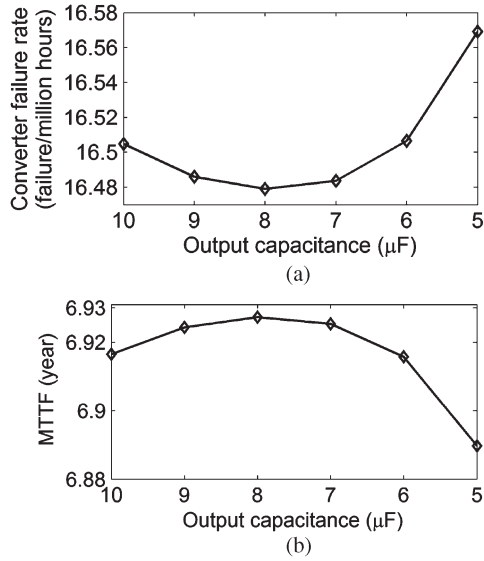
Fig. 7. (a) Converter failure rate versus output capacitance C. (b) MTTF of the converter versus output capacitance C.

Fig. 8. (a) Converter failure rate versus ESR and C. (b) MTTF of the converter versus ESR.

Change in Capacitance (C)

The effect of capacitance variation on the reliability and the MTTF of the converter is discussed in this section. The output capacitance of the converter was varied from 10 to 5 μF in steps of 1 μF. $R_{DS(\mathrm{ON})}$ and ESR were set to 34 mΩ and 0.1 Ω, respectively. The failure of an aluminum electrolytic capacitor is shown in (13) as follows:

$$\lambda_{\mathrm{CAP0}} = \lambda_{b0}\pi_{\mathrm{CV0}}\pi_E\pi_Q$$

$$\lambda_{b0} = \text{base failure rate}$$

$$= 0.0028 \times \left[\left(\frac{S_{\mathrm{CAP}}}{0.55}\right)^3 + 1\right]\exp\left(4.09\left(\frac{T+273K}{358K}\right)^{5.9}\right)$$

$$\pi_{\mathrm{CV0}} = \text{capacitance factor} = 0.32(C\mu\mathrm{F})^{0.19}. \tag{13}$$

Here, λ_b is the base failure rate and is a function of ripple voltage across the capacitor. S_{CAP} is ratio of the operating voltage to the rated voltage, and rated voltage is defined as the sum of applied average dc voltage and peak ac voltage. T is the ambient temperature. π_{CV} is the capacitance factor and depends on the capacitance of the capacitor.

Starting from 10 μF, decreasing capacitance increases voltage ripple across the capacitor and thereby increases the base failure rate. However, the capacitance factor decreases with any decrease in capacitance. Therefore, the failure rate of the converter decreases with any reduction in capacitance and starts to increase when the base failure rate becomes dominant over the capacitance factor. The failure rate and the MTTF of the converter versus output capacitance is shown in Fig. 7. The MTTF of the converter is reduced by about 330 h for the variation in C from 10 to 5 μF. However, any variation in the output capacitance does not have any significant effect on the failure rates of other components of the converter.
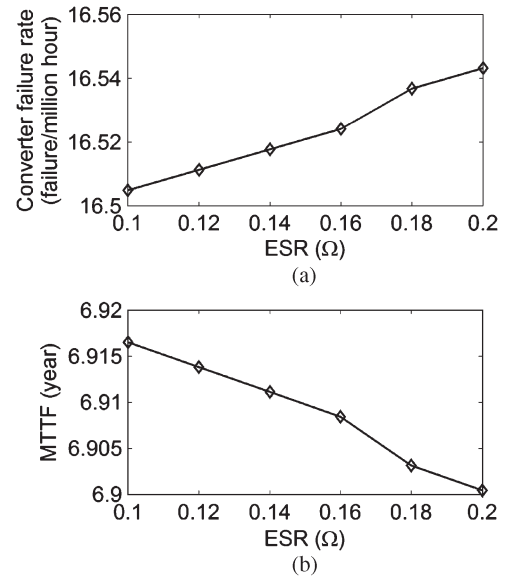
Change in ESR of the Output Capacitor

The effect of capacitor's ESR on the reliability and MTTF of the converter is discussed in this section. The ESR of the output capacitor was varied from 0.1 to 0.2 Ω in steps of 0.02 Ω. $R_{DS(\mathrm{ON})}$ and C were set to 34 mΩ and 10 μF, respectively. Similar to $R_{DS(\mathrm{ON})}$ variation, the failure rate of the converter increases with any increase in the ESR. However, the failure rate of the converter is less sensitive to the ESR compared with $R_{DS(\mathrm{ON})}$. The failure rate and MTTF of the converter versus ESR is shown in Fig. 8. The MTTF of the converter is reduced by approximately 140 h for the variation in the ESR ranging from 0.1 to 0.2 Ω.

V. EXPERIMENTAL ANALYSIS

This section presents an experimental analysis to study the operation of a boost converter with open-loop control and closed-loop control from the reliability perspective. An off-the-shelf boost converter shown in Fig. 9(a) has been used for this purpose [40]. This converter has a 1000-μF capacitor connected at the output and a MOSFET (STB75NF75) with $R_{DS(\mathrm{ON})}$ equal to 8.41 mΩ measured at gate voltage and drain current equal to 12 V and 4 A, respectively. The control circuit of the converter was disconnected, and an external gate signal has been provided on purpose. Three different test cases of the converter's operation have been studied, as discussed in the following.

Test Case 1—Operation With the New Converter

The boost converter was operated at switching frequency of 100 kHz, and the input voltage was fixed to 15 V. The output was connected to a dc electronic load with fixed load resistance equal to 6 Ω. The boost converter was operating in CCM, and a screenshot of the output voltage, voltage across the
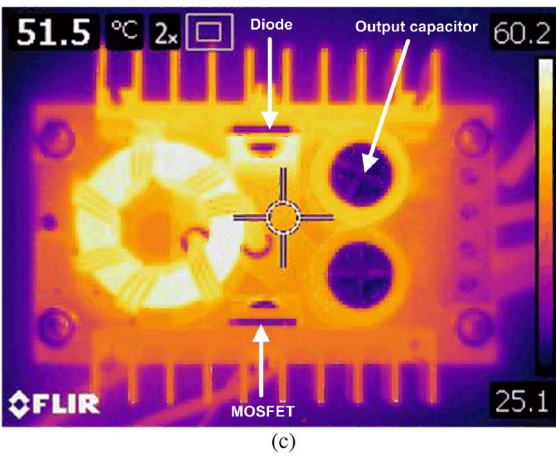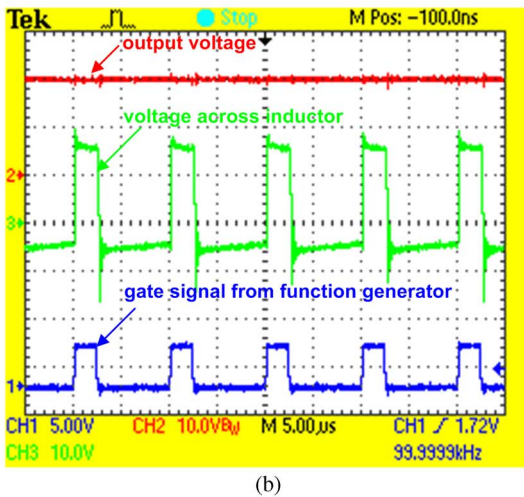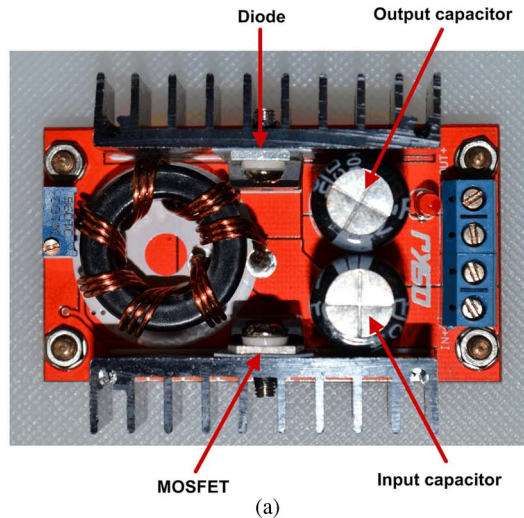
(a)

(b)

(c)

Fig. 9.   (a) Boost converter. (b) Oscilloscope capture of gate signal, voltage across the inductor, and the output voltage. (c) Thermal image of the boost converter.

inductor, and the gate signal generated by the arbitrary signal generator (GW INSTEK AFG-2125) is shown in Fig. 9(b). The output voltage of the converter was 19.02 V with a duty ratio equal to 23.4%. The thermal image of the converter was taken using a FLIR T420 infrared camera and is shown in Fig. 9(c). Details of other experimental parameters have been listed in Table II.

TABLE II
DIFFERENT PARAMETERS OF THE EXPERIMENTAL TESTS
WITH THE COMMERCIAL BOOST CONVERTER

	Test case 1 (reference)	Test case 2 (open loop with increased $R_{DS(ON)}$)	Test case 3 (closed loop with increased $R_{DS(ON)}$)
Input voltage	15 V	15 V	15 V
Input current	4.28 A	4.15 A	4.30 A
Output voltage	19.02 V	18.68 V	19.02 V
Output load resistance	6 Ω	6 Ω	6 Ω
Output power	60.3 W	58.2 W	60.3 W
Output voltage ripple	~ 75 mV	~ 75 mV	~ 75 mV
Duty ratio	23.4 %	23.4 %	24.7%
MOSFET $R_{DS(ON)}$ (at V_{GS} =12V and I_d = 4 A)	8.41 mΩ	25.45 mΩ	25.45 mΩ
MOSFET's case temperature	44.6 °C	40.4 °C	45.3 °C
Ambient temperature	25 °C	25 °C	25 °C
Switching frequency	100 kHz	100 kHz	100 kHz

Test Case 2—Operation With MOSFET of Higher $R_{DS(ON)}$ and Open-Loop Control

In order to demonstrate the impact of higher $R_{DS(ON)}$, the MOSFET of the converter has been replaced by IRFZ34 with $R_{DS(ON)}$ equal to 25.45 mΩ measured at gate voltage and drain current equal to 12 V and 4 A, respectively. The output voltage of the converter dropped to 18.68 V for the same input voltage, duty ratio, and output load resistance, as described in test case 1. This operation is similar to open-loop control where the duty cycle is not changed with the variation of the output voltage of the converter since input voltage is fixed to 15 V.

Test Case 3—Operation With MOSFET of Higher $R_{DS(ON)}$ and Closed-Loop Control

The duty cycle of the converter was increased to 24.7% to achieve 19.02 V at the output, and it resembles the operation of the boost converter in closed loop.

During all the test cases, the ambient temperature was fixed to 25 °C in the laboratory setup, and no forced cooling has been provided. The output voltage ripple was ∼75 mV.

TABLE III
SYSTEM FAILURE RATE FOR CHARACTERISTICS VARIATION OF $R_{DS(ON)}$, C, AND ESR

$R_{DS(ON)}$ (mΩ) with C=10μF, ESR=0.1Ω	System failure rate (λ_{SYSTEM}) (failure/ million- hours)	Capacitance (μF) with $R_{DS(ON)}$ = 34 mΩ ESR=0.1 Ω	System failure rate (λ_{SYSTEM}) (failure/ million- hours)	ESR (Ω) with C=10 μF, $R_{DS(ON)}$ = 34 mΩ	System failure rate (λ_{SYSTEM}) (failure/ million- hours)
34	16.5048	10	16.5048	0.10	16.5048
36	16.6294	9	16.4860	0.12	16.5112
38	16.7551	8	16.4789	0.14	16.5177
40	16.8817	7	16.4836	0.16	16.5241
42	17.0094	6	16.5065	0.18	16.5367
44	17.1380	5	16.5690	0.20	16.5432

Test case 1 has been performed to get a reference for open-loop control and closed-loop control with increased $R_{DS(ON)}$. The output voltage drops with an increase in $R_{DS(ON)}$ during test case 2. Since the ambient temperature T in (13) was fixed to 25 °C, decreased voltage stress across the output capacitor will result in smaller failure rate λ_{CAP0}. Moreover, the power loss in the MOSFET was decreased due to smaller input current (4.15 A) compared with 4.28 A in test case 1. The case temperature of the MOSFET was decreased from 44.6 °C to 40.4 °C. Therefore, these observations agree with the fact that increased ON-state resistance of the MOSFET in an open-loop boost converter will increase the reliability of the entire power converter since the MOSFET and the capacitor are the most failure-prone components here [2].

It is shown in Section IV that increased $R_{DS(ON)}$ results in higher duty ratio d and, consequently, higher power loss in the MOSFET in closed-loop operation of the converter. Similar results have been observed in test case 3 as the duty ratio increased from 23.4% (test case 1) to 24.7% to maintain the output voltage fixed to 19.02 V. An increased duty ratio has resulted in higher power loss across the MOSFET (case temperature increased from 44.6 °C to 45.3 °C). Moreover, there is no change in the failure rate of the output capacitor since the voltage stress and the ambient temperature were same in both test cases 1 and 3. Therefore, it can be concluded that increased $R_{DS(ON)}$ of the MOSFET in a closed-loop boost converter will not increase the reliability of the entire power converter.

VI. CONCLUSION AND FUTURE WORK

Reliability degradation of a boost converter being operated in closed loop has been presented in this paper. Components used in this converter exhibit parameter variations due to aging of the entire converter. Therefore, the effect of any variation in MOSFET ON-state resistance $R_{DS(ON)}$, capacitance C, and ESR of the output capacitor on the reliability of the power converter have been analyzed, and a summary is presented in Table III. The MTTF of the closed-loop converter decreases with the gradual increase in both $R_{DS(ON)}$ and ESR. However, any variation in $R_{DS(ON)}$ significantly impacts the reliability of the entire converter compared with C and ESR. In addition, the reliability of the converter varies in a more complex manner

while it is expressed as a function of the capacitance C. However, the impact of any variation associated to one component on the remaining components has been studied as well. We believe that this technique could be applied to many other high-power converters where predicting the failure rate and reliability is critical. Implementation of a complete prognostics and health monitoring system with appropriate *in situ* measurements will be addressed in future.

REFERENCES

[1] *Military Handbook: Reliability Prediction of Electronic Equipment*, Dept. Defense, Washington, DC, USA, Dec. 2, 1991, MIL-HDBK-217F.

[2] S. V. Dhople, A. Davoudi, A. D. Domínguez-García, and P. L. Chapman, "A unified approach to reliability assessment of multiphase DC-DC converters in photovoltaic energy conversion systems," *IEEE Trans. Power Electron.*, vol. 27, no. 2, pp. 739–751, Feb. 2012.

[3] *Military Handbook: Electronic Reliability Design Handbook*, Dept. Defense, Washington, DC, USA, Oct. 12, 1998, MIL-HDBK-338B.

[4] A. Testa, S. De Caro, and S. Russo, "A reliability model for power MOSFETs working in avalanche mode based on an experimental temperature distribution analysis," *IEEE Trans. Power Electron.*, vol. 27, no. 6, pp. 3093–3100, Jun. 2012.

[5] *Reliability Centered Maintenance Guide for Facilities and Collateral Equipment*, National Aeronautics and Space Admin. (NASA), Washington, DC, USA, 2000.

[6] G. P. Sullivan, R. Pugh, A. P. Melendez, and W. D. Hunt, *Operations & Maintenance Best Practices: A Guide to Achieving Operational Efficiency*. Richland, WA, USA: Pacific Northwest National Laboratory, Aug. 2010, Federal Energy Management Program U.S. Department of Energy, release 3.0.

[7] J. Piotrowski, Pro-active maintenance for pumps, archives, February 2001, Pump-Zone.com, Birmingham, AL, USA. [Online]. Available: http://www.pump-zone.com

[8] G. A. Klutke, P. C. Kiessler, and M. A. Wortman, "A critical look at the bathtub curve," *IEEE Trans. Rel.*, vol. 52, no. 1, pp. 125, 129, Mar. 2003.

[9] M. A. Moss, *Designing for Minimal Maintenance Expense: The Practical Application of Reliability and Maintainability*. New York, NY, USA: Marcel Dekker, 1985.

[10] R. Burgos *et al.*, "Reliability-oriented design of three-phase power converters for aircraft applications," *IEEE Trans. Aerosp. Electron. Syst.*, vol. 48, no. 2, pp. 1249, 1263, Apr. 2012.

[11] S. Yang *et al.*, "An industry-based survey of reliability in power electronic converters," *IEEE Trans. Ind. Appl.*, vol. 47, no. 3, pp. 1441, 1451, May/Jun. 2011.

[12] S. E. De León-Aldaco, H. Calleja, F. Chan, and H. R. Jiménez-Grajales, "Effect of the mission profile on the reliability of a power converter aimed at photovoltaic applications—A case study," *IEEE Trans. Power Electron.*, vol. 28, no. 6, pp. 2998, 3007, Jun. 2013.

[13] B. Abdi, A. H. Ranjbar, J. Milimonfared, and G. B. Gharehpetian, "Reliability comparison of boost PFC converter in DCM and CCM operating modes," in *Proc. Int. SPEEDAM*, Jun. 11–13, 2008, pp. 939, 943.

[14] F. Chan and H. Calleja, "Reliability estimation of three single-phase topologies in grid-connected PV systems," *IEEE Trans. Ind. Electron.*, vol. 58, no. 7, pp. 2683, 2684, Jul. 2011.

[15] S. Harb and R. S. Balog, "Reliability of candidate photovoltaic module-integrated-inverter topologies," in *Proc. 27th Annu. IEEE APEC Expo.*, Feb. 5–9, 2012, pp. 898, 903.

[16] A. L. Julian and G. Oriti, "A comparison of redundant inverter topologies to improve voltage source inverter reliability," *IEEE Trans. Ind. Appl.*, vol. 43, no. 5, pp. 1371, 1378, Sep./Oct. 2007.

[17] H. Wang, D. Zhou, and F. Blaabjerg, "A reliability-oriented design method for power electronic converters," in *Proc. Annu. IEEE 28th APEC Expo.*, Mar. 17–21, 2013, pp. 2921, 2928.

[18] S. K. Mazumder and K. Shenai, "On the reliability of distributed power systems: A macro- to microlevel overview using a parallel DC-DC converter," in *Proc. 33rd IEEE PESC*, 2002, vol. 2, pp. 809, 814.

[19] M. P. Pecht, *Health Management of Electronics*. New York, NY, USA: Wiley-Interscience, 2008.

[20] S. Cheng, K. Tom, and M. Pecht, "Failure precursors for polymer resettable fuses," *IEEE Trans. Device Mater. Rel.*, vol. 10, no. 3, pp. 374, 380, Sep. 2010.

[21] E. Wolfgang, "Examples for failures in power electronics systems," ECPE Tutorial Reliability Power Electronic Systems, Nuremberg, Germany, Apr. 2007.

[22] M. S. Nasrin and F. H. Khan, "Real time monitoring of aging process in power converters using the sSTDR generated impedance matrix," in *Proc. IEEE APEC Expo.*, 2013, pp. 1199–1205.

[23] S. Yang *et al.*, "An industry-based survey of reliability in power electronic converters," in *Proc. IEEE ECCE*, Sep. 20–24, 2009, pp. 3151, 3157.

[24] S. Yang *et al.*, "Condition monitoring for device reliability in power electronic converters: A review," *IEEE Trans. Power Electron.*, vol. 25, no. 11, pp. 2734, 2752, Nov. 2010.

[25] H. Wang, K. Ma, and F. Blaabjerg, "Design for reliability of power electronic systems," in *Proc. 38th IEEE IECON*, Oct. 25–28, 2012, pp. 33, 44.

[26] N. Mohan, T. M. Undeland, and W. P. Robbins, *Power Electronics: Converters, Applications, Design*, 3rd ed. Hoboken, NJ, USA: Wiley, 2003.

[27] M. H Rashid, *Power Electronics—Devices, Circuits and Applications*. Cambridge, U.K.: Pearson, 2014.

[28] L. Jing, Y. Xiaobin, and F. Peiyun, "Improved small signal modeling and analysis of the PI controlled boost converter," in *Proc. ICECC*, Sep. 9–11, 2011, pp. 3763, 3767.

[29] W. Stefanutti, P. Mattavelli, S. Saggini, and M. Ghioni, "Autotuning of digitally controlled DC-DC converters based on relay feedback," *IEEE Trans. Power Electron.*, vol. 22, no. 1, pp. 199, 207, Jan. 2007.

[30] W.-H. Chang, H.-S. Nien, and C.-H. Chen, "A digital boost converter to drive white LEDs," in *Proc. 23rd Annu. IEEE APEC Expo.*, Feb. 24–28, 2008, pp. 558, 564.

[31] J. Morroni, R. Zane, and D. Maksimovic, "An online stability margin monitor for digitally controlled switched-mode power supplies," *IEEE Trans. Power Electron.*, vol. 24, no. 11, pp. 2639, 2648, Nov. 2009.

[32] B. J. Patella, A. Prodic, A. Zirger, and D. Maksimovic, "High-frequency digital PWM controller IC for DC-DC converters," *IEEE Trans. Power Electron.*, vol. 18, no. 1, pp. 438, 446, Jan. 2003.

[33] V. Arikatla and J. A. Abu-Qahouq, "An adaptive digital PID controller scheme for power converters," in *Proc. IEEE ECCE*, Sep. 12–16, 2010, pp. 223, 227.

[34] Y.-X. Wang, D.-H. Yu, and Y.-B. Kim, "Robust time-delay control for the DC-DC boost converter," *IEEE Trans. Ind. Electron.*, vol. 61, no. 9, pp. 4829, 4837, Sep. 2014.

[35] S. Saha, R. C. Jose, V. Vashchenko, S. Mahiuddin, and F. G. Kai, "Accelerated aging with electrical overstress and prognostics for power MOSFETs," in *Proc. IEEE Energytech*, 2011, pp. 1–6.

[36] J. R. Celaya, A. Saxena, C. S. Kulkarni, S. Saha, and K. Goebel, "Prognostics approach for power MOSFET under thermal-stress aging," in *Proc. Annu. RAMS*, 2012, pp. 1–6.

[37] *Application Note AN-0994: Maximizing the Effectiveness of your SMD Assemblies*, International Rectifier, El Segundo, CA, USA, May 2012.

[38] K.-W. Lee, M. Kim, J. Yoon, S. B. Lee, and J.-Y. Yoo, "Condition monitoring of DC-link electrolytic capacitors in adjustable-speed drives," *IEEE Trans. Ind. Appl.*, vol. 44, no. 5, pp. 1606–1613, Sep./Oct. 2008.

[39] M. S. Nasrin and F. H. Khan, "Characterization of aging process in power converters using spread spectrum time domain reflectometry," in *Proc. IEEE ECCE*, Sep. 15–20, 2012, pp. 2142–2148.

[40] Accessed on March 31, 2014. [Online]. Available: http://www.amazon.com/gp/product/B00EC86X8O/ref=oh_details_o02_s00_i00?ie=UTF8&psc=1

Mohammed Khorshed Alam (S'11) received the B.S. degree in electrical and electronic engineering from Bangladesh University of Engineering and Technology, Dhaka, Bangladesh, in 2009. He is currently working toward the Ph.D. degree in electrical engineering at the University of Utah, Salt Lake City, UT, USA.

From 2009 to 2010, he was a Lecturer with Ashanullah University of Science and Technology, Dhaka, Bangladesh. His research interests include renewable energy harvesting, high-power switched-capacitor converters, low-power circuits for biological implants and sensors, and fault detection and reliability analysis of power converters.

Faisal H. Khan (SM'13) received the B.Sc. degree from Bangladesh University of Engineering and Technology, Dhaka, Bangladesh, in 1999, the M.S. degree from Arizona State University, Phoenix, AZ, USA, in 2003, and the Ph.D. degree from the University of Tennessee, Knoxville, TN, USA, in 2007, all in electrical engineering.

From 2007 to 2009, he has been with the Electric Power Research Institute as a Senior Power Electronics Engineer. Since 2009, he has been with the Department of Electrical and Computer Engineering, University of Utah, Salt lake City, UT, USA, as an Assistant Professor.

Dr. Khan serves as an Associate Editor of the IEEE TRANSACTIONS ON POWER ELECTRONICS.